

AN INFRARED SURVEY OF BRIGHTEST CLUSTER GALAXIES. II. WHY ARE SOME BRIGHTEST CLUSTER GALAXIES FORMING STARS?

CHRISTOPHER P. O’DEA, STEFI A. BAUM, GEORGE PRIVON, AND JACOB NOEL-STORR

Department of Physics, Rochester Institute of Technology, 84 Lomb Memorial Drive, Rochester, NY 14623-5603;
odea@cis.rit.edu, baum@cis.rit.edu, gcp1035@cis.rit.edu, jake@cis.rit.edu

ALICE C. QUILLEN, NICHOLAS ZUFELT, AND JAEHONG PARK

Department of Physics and Astronomy, University of Rochester, Rochester, NY 14627;
zufelt72@potsdam.edu, jaehong@pas.rochester.edu, aquillen@pas.rochester.edu

ALASTAIR EDGE

Institute for Computational Cosmology, Department of Physics, Durham University,
Durham DH1 3LE, UK; alastair.edge@durham.ac.uk

HELEN RUSSELL AND ANDREW C. FABIAN

Institute of Astronomy, Madingley Road, Cambridge CB3 0HA, UK; hrr27@ast.cam.ac.uk, acf@ast.cam.ac.uk

MEGAN DONAHUE

Physics and Astronomy Department, Michigan State University,
East Lansing, MI 48824-2320; donahue@pa.msu.edu

CRAIG L. SARAZIN

Department of Astronomy, University of Virginia, P.O. Box 400325,
Charlottesville, VA 22904-4325; cls7i@mail.astro.virginia.edu

BRIAN MCNAMARA

Department of Physics and Astronomy, University of Waterloo, 200 University Avenue West,
Waterloo, ON N2L 3G1, Canada; mcnamara@uwaterloo.ca

JOEL N. BREGMAN

Physics Department, University of Michigan, Ann Arbor, MI 48109; jbregman@umich.edu

AND

EIICHI EGAMI

Steward Observatory, University of Arizona, 933 North Cherry Avenue,
Tucson, AZ 85721; eegami@as.arizona.edu

Received 2007 November 23; accepted 2008 March 11

ABSTRACT

Quillen et al. presented an imaging survey with the *Spitzer Space Telescope* of 62 brightest cluster galaxies with optical line emission located in the cores of X-ray-luminous clusters. They found that at least half of these sources have signs of excess IR emission. Here we discuss the nature of the IR emission and its implications for cool core clusters. The strength of the mid-IR excess emission correlates with the luminosity of the optical emission lines. Excluding the four systems dominated by an AGN, the excess mid-IR emission in the remaining brightest cluster galaxies is likely related to star formation. The mass of molecular gas (estimated from CO observations) is correlated with the IR luminosity as found for normal star-forming galaxies. The gas depletion timescale is about 1 Gyr. The physical extent of the IR excess is consistent with that of the optical emission-line nebulae. This supports the hypothesis that star formation occurs in molecular gas associated with the emission-line nebulae and with evidence that the emission-line nebulae are mainly powered by ongoing star formation. We find a correlation between mass deposition rates (\dot{M}_X) estimated from the X-ray emission and the star formation rates estimated from the IR luminosity. The star formation rates are 1/10 to 1/100 of the mass deposition rates, suggesting that the reheating of the intracluster medium is generally very effective in reducing the amount of mass cooling from the hot phase but not eliminating it completely.

Subject headings: cooling flows — galaxies: active — galaxies: clusters: general —
galaxies: elliptical and lenticular, cD — infrared: galaxies — stars: formation

1. INTRODUCTION

The hot $T \sim 10^7 - 10^8$ K X-ray-emitting gas is currently thought to constitute the bulk of the baryonic mass in rich clusters of galaxies. An important aspect of the overall physics of the intracluster medium (ICM) concerns the central regions of clusters ($r \lesssim 10 - 100$ kpc), where the inferred ICM densities and pressures in some cases are sufficiently high that cooling to $T \lesssim 10^4$ K can occur on timescales shorter than the cluster lifetime (e.g., Cowie

& Binney 1977; Fabian & Nulsen 1977; Edge et al. 1992). These “cooling core” clusters often exhibit intense optical emission-line nebulae associated with the centrally dominant (cD) galaxies at their centers, together with blue continuum excess emission, and the strength of these effects appears to correlate with the cooling rate or central pressure of the X-ray-emitting gas (Heckman 1981; Johnstone & Fabian 1987; Romanishin 1987; McNamara & O’Connell 1992, 1993; Crawford & Fabian 1992, 1993; Allen 1995).

The previous paradigm pictured the ICM as a relatively simple place where gas cooled and slumped in toward the center of the cluster in a cooling flow with mass accretion rates of hundreds of solar masses per year (e.g., Fabian 1994). However, X-ray spectroscopy with *XMM-Newton* and *Chandra* has failed to find evidence for gas at temperatures below about one-third of the cluster virial temperature (e.g., Kaastra et al. 2001; Tamura et al. 2001; Peterson et al. 2001, 2003; Peterson & Fabian 2006). The limits on the luminosity of the intermediate-temperature gas imply reductions in the inferred mass accretion rates by factors of 5–10. Recent theoretical models indicate that intracluster conduction, combined with an episodic heat source in the cluster core, such as an AGN or star formation, are candidates for explaining both the X-ray emission from cluster cores and the optical emission-line phenomena associated with the cores with these rapidly cooling spectra (e.g., Ruszkowski & Begelman 2002; Voigt et al. 2002; Fabian et al. 2002; Narayan & Medvedev 2001). One widely considered possibility is that an important source of heat in the ICM is bubbles driven by radio galaxies (e.g., Baum & O’Dea 1991; Tucker & David 1997; Soker et al. 2002; Böhringer et al. 2002; Kaiser & Binney 2003; Omma et al. 2004; Dunn et al. 2005; Dunn & Fabian 2006; Birzan et al. 2004; Rafferty et al. 2006), which halt the cooling of the gas. The ICM now appears to be a very dynamic place where heating and cooling processes vie for dominance and an uneasy balance is maintained. Since these same processes may operate during the process of galaxy formation, the centers of clusters of galaxies provide low-redshift laboratories for studying the critical processes involved in galaxy formation and supermassive black hole growth. At the present time, the main questions are (1) how much gas is cooling out of the ICM? (2) how much star formation is ongoing? and (3) what is the impact of the gas and star formation on the central brightest cluster galaxy (BCG)?

As little mass is needed to power the AGNs at the centers of bright cluster galaxies, the only way to remove cooled gas from the ICM is to form stars. Measurements of the star formation rate (SFR) in cluster galaxies can therefore provide constraints on the efficiency of cooling, the fraction of gas that cools, and the needed energy input to prevent the remainder of the gas from cooling. It is also possible that the ICM in cluster galaxies is not in a steady state or experiencing periods of enhanced cooling and star formation and periods of relative activity when cooling is prevented. Star formation and associated supernovae also provide a source of mechanical energy, although this is not sufficient to match the X-ray radiative energy losses (McNamara et al. 2006).

ISO observations detected the cluster Sérsic 159-03 (Hansen et al. 2000). Recent *Spitzer* observations have demonstrated that star formation is common in cooling core BCGs (Egami et al. 2006b; Donahue et al. 2007b; Quillen et al. 2008, hereafter Paper I). An IR excess is found in about half of the sample of 62 BCGs studied by Paper I. In this paper we discuss the results of Paper I. We examine correlations in the data and discuss the implications for star formation in BCGs and the balance of heating and cooling in the ICM. Specifically, we search for correlations between SFRs, radio, $H\alpha$, CO, and X-ray luminosities and mass deposition rates estimated from the X-ray observations. In this paper all luminosities have been corrected or computed to be consistent with a Hubble constant $H_0 = 70 \text{ Mpc}^{-1} \text{ km s}^{-1}$ and a concordance cosmology ($\Omega_M = 0.3$ and flat).

2. COMPARISON DATA

The properties of the BCG sample are discussed by Paper I. Comparison data for the BCGs in our sample are listed in Table 1

TABLE 1
SPEARMAN RANK ORDER CORRELATION COEFFICIENTS

Plot Name (1)	Figure Number (2)	Correlation Coefficient (3)	Two-sided Significance (4)
L_X vs. L_{IR}	2	0.63	5.0×10^{-5}
F_X vs. F_{IR}	0.14	0.40
L_X vs. $8/5.8$	3	0.38	3×10^{-3}
$L_{1.4 \text{ GHz}}$ vs. L_{IR}	4	0.41	0.02
$F_{1.4 \text{ GHz}}$ vs. F_{IR}	-0.09	0.61
$L_{H\alpha}$ vs. L_{IR}	5	0.91	3.6×10^{-12}
$F_{H\alpha}$ vs. F_{IR}	0.65	1.1×10^{-4}
$L(H\alpha)$ vs. $L(24 \mu\text{m})$	0.84	2×10^{-15}
$F(H\alpha)$ vs. $F(24 \mu\text{m})$	6	0.67	4×10^{-8}
$M(H_2)$ vs. L_{IR}	7	0.95	1.3×10^{-10}
$F(CO)$ vs. F_{IR}	0.81	1.7×10^{-5}

NOTES.—Col. (1): Correlation being tested. Col. (2): Figure that plots the data. Col. (3): Spearman rank order correlation coefficients. Col. (4): Two-sided significance of the correlation’s deviation from zero. The most significant correlations are that between $H\alpha$ and IR luminosity and that between molecular gas mass and IR luminosity. Most correlations are done on both fluxes and luminosities.

of Paper I. When available, this table lists X-ray (primarily *ROSAT* 0.1–2.4 keV), radio (1.4 GHz), and $H\alpha$ luminosities (from long-slit spectra and SDSS data) and $[O \text{ III}] \lambda 5007/H\beta$ flux ratios. BCGs can host both star formation and an AGN. X-ray luminosities provide a constraint on the mass in and radiative losses from the hot ICM. The $H\alpha$ recombination line is excited by emission from hot stars produced during formation or from an AGN. We note that emission lines are detected in $\sim 10\%$ – 20% of typical optically selected BCGs, $\sim 30\%$ – 40% of X-ray-selected BCGs, and almost 100% of BCGs in cooling core clusters (Donahue et al. 1992; Crawford et al. 1999; Best et al. 2007; Edwards et al. 2007). To discriminate between the presence of an AGN and star formation, we have sought a measure of the hardness of the radiation field through the $[O \text{ III}] \lambda 5007/H\beta$ optical line ratio. Fluxes in the radio also provide a constraint on the properties of the AGN. Below we discuss SFRs estimated using IR luminosities derived from aperture photometry listed in Paper I, molecular gas masses estimated from CO observations, and mass deposition rates measured from X-ray observations. The statistical tests for correlations between the various quantities are given in Table 1.

3. ESTIMATED STAR FORMATION RATES

If the IR luminosity is powered by star formation, we can use the IR luminosity to estimate an SFR (e.g., Bell 2003; Calzetti 2008). But first we need to consider whether some sources have a contribution to the IR from a type II AGN with an optically bright accretion disk. Paper I identified Z2089, A1068, and A2146 as likely to have an AGN contribution based on red $4.5/3.6 \mu\text{m}$ color, an unresolved nucleus seen in IRAC color maps, and a high $[O \text{ III}]/H\beta$ flux ratio. R0821+07 was flagged as possibly similar, as it has an unresolved nucleus in IRAC color maps and a high $[O \text{ III}]/H\beta$. It also has a remarkably red $8.0/5.6 \mu\text{m}$ color similar to a Seyfert 2 with an embedded dusty AGN. In Figure 1 we plot the ratio of 4.5 and $3.6 \mu\text{m}$ fluxes to redshift (data from Paper I). The clear trend seen is as expected for a passive stellar population but with a few notable exceptions. The sources with strong $[O \text{ III}]$ (Z2089, A1068, and A2146) lie above the trend, as do A2055 and A2627, which show evidence for a BL Lac continuum in optical spectra (Crawford et al. 1999). The two galaxies

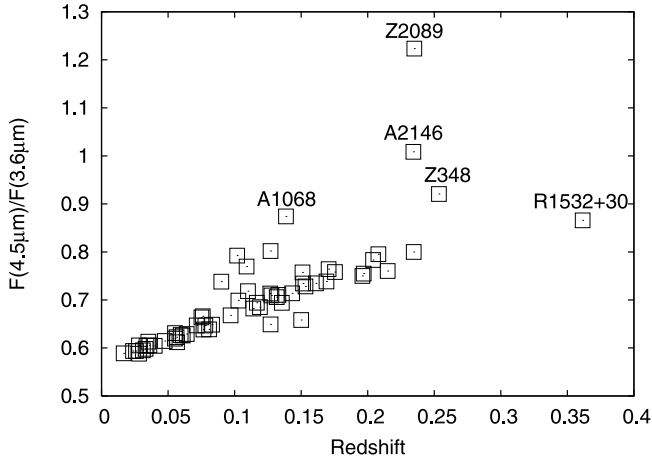


FIG. 1.—Flux ratio $F_{4.5 \mu\text{m}}/F_{3.6 \mu\text{m}}$ vs. redshift. The labeled objects show evidence for the presence of an optically luminous type II AGN.

that lie below the trend are Z2072 and Z9077 and are among the fainter objects in our sample. Z9077 was the only object not detected at $24 \mu\text{m}$. The four that are between $z = 0.09$ and 0.15 and lie slightly above the trend are A1885, A2055, A2627, and R0352+19. It is not obvious why these four sources lie above the trend or whether this is significant. R0352+19 and R0821+07 are quite red in the $8.0/5.8 \mu\text{m}$ color, and R1532+30 and Z348 are pretty red in $8.0/5.8 \mu\text{m}$ but do not stand out in the $4.5/3.6 \mu\text{m}$ color versus z plot. Thus, the combination of diagnostics ($4.5/3.6 \mu\text{m}$ color, red unresolved nuclear source, and high $[\text{O III}]/\text{H}\beta$ ratio) identifies some sources with a strong AGN contribution. The remaining objects are likely to be free of strong AGN contamination.

Previous optical and UV observations have found evidence for significant star formation in the BCGs in cool core clusters (Johnstone & Fabian 1987; Romanishin 1987; McNamara & O’Connell 1989, 1993; McNamara 2004; McNamara et al. 2004; Hu 1992; Crawford & Fabian 1993; Hansen et al. 1995; Allen 1995; Smith et al. 1997; Cardiel et al. 1998; Hutchings & Balogh 2000; Oegerle et al. 2001; Mittaz et al. 2001; O’Dea et al. 2004; Hicks & Mushotzky 2005; Rafferty et al. 2006). Table 1 of Paper I lists $[\text{O III}]/\text{H}\beta$ ratios for most of the BCGs. Except for the few which may host an AGN, the ratios are consistent with the gas being ionized by hot stars.

In Table 2 we present the estimated IR luminosities from Paper I and the estimated SFRs. The SFR can be estimated from the IR luminosity with equation (5) of Bell (2003),

$$\psi(M_{\odot} \text{ yr}^{-1}) = A \left(\frac{L_{\text{IR}}}{L_{\odot}} \right) \left(1 + \sqrt{10^9 L_{\odot}/L_{\text{IR}}} \right). \quad (1)$$

Here the constant $A = 1.57 \times 10^{-10}$ for $L_{\text{IR}} > 10^{11} L_{\odot}$ and $A = 1.17 \times 10^{-10}$ at lower luminosities. The SFRs are in the range of about 1 to a few tens of $M_{\odot} \text{ yr}^{-1}$. The objects with SFRs above about $50 M_{\odot} \text{ yr}^{-1}$ are likely AGN-dominated.

In Table 3 we list available SFRs in different wave bands. We see that there is dispersion in the estimated SFRs. However, because of the effects of dust and geometry we do not necessarily expect agreement between SFRs estimated in the IR versus the UV/optical. Much of the variation can be accounted for by aperture mismatch; differences in assumptions about star formation history, i.e., burst versus constant star formation; extinction; and perhaps differences in the amount of dust available to reradiate in the far-IR (FIR). Note that A1068 and A2146 show large discrepancies between our FIR SFR and the U -band SFR, and both

TABLE 2
STAR FORMATION RATE

Cluster	L_{IR} ($10^{44} \text{ erg s}^{-1}$)	SFR ($M_{\odot} \text{ yr}^{-1}$)
Z2089*	64.68	271
A2146*	45.46	192
A1068*	44.61	188
R0821+07*	8.47	37
R1532+30*	22.62	97
Z8193*	13.70	59
Z0348*	11.92	52
A0011*	7.97	35
PKS 0745–1	3.80	17.2
A1664	3.21	14.6
R0352+19	2.40	11.1
NGC 4104	0.80	4.0
R0338+09	0.39	2.1
R0439+05*	4.17	18.7
A2204	3.23	14.7
A2627	1.59	7.5
A0115	1.30	6.2
Z8197	0.72	3.6
R2129+00	2.93	13.4
A1204	1.73	8.1
A0646	1.49	7.1
A2055	1.46	7.0
A0291	1.30	6.3
A1885	1.04	5.1
A3112	0.84	4.2
A2292	0.80	4.0
A1930	0.75	3.8
Z8276	0.74	3.7
A4095	0.29	1.6
A0085	0.28	1.6
A2052	0.24	1.4
R0000+08	0.20	1.2
NGC 6338	0.18	1.0
R0751+50	0.10	0.65
A0262	0.08	0.54

NOTES.—IR luminosities are from Paper I, estimated from the $15 \mu\text{m}$ wavelength for BCGs that are detected at $70 \mu\text{m}$ or have color ratios $F_{8 \mu\text{m}}/F_{5.8 \mu\text{m}} > 1.0$ or $F_{24 \mu\text{m}}/F_{8 \mu\text{m}} > 1.0$. The SFR was estimated using eq. (1). The top section contains four BCGs that are suspected to harbor dusty type II AGNs. Z2089, A2146, and A1068 exhibit a red $F_{4.5 \mu\text{m}}/F_{3.6 \mu\text{m}}$ color, and all four exhibit high $[\text{O III}]\lambda 5007/\text{H}\beta$ flux ratios. Note that if there is an AGN present in one of these clusters, the SFR may be overestimated. The second section contains the remaining nine BCGs with $F_{8 \mu\text{m}}/F_{5.8 \mu\text{m}} > 1.3$. The third section contains the set of five clusters with $1.0 < F_{8 \mu\text{m}}/F_{5.8 \mu\text{m}} < 1.3$. The fourth section contains the remaining BCGs with IR excesses. Specifically, they have ratios $F_{8 \mu\text{m}}/F_{5.8 \mu\text{m}} > 1.0$, $F_{24 \mu\text{m}}/F_{8.0 \mu\text{m}} > 1.0$, or a detected $70 \mu\text{m}$ flux. The BCGs marked with an asterisk can be classified as LIRGs since they have L_{IR} greater than $10^{11} L_{\odot}$. Objects with $F_{8 \mu\text{m}}/F_{5.8 \mu\text{m}} < 1.0$ or $F_{24 \mu\text{m}}/F_{8 \mu\text{m}} < 1$ and lacking a $70 \mu\text{m}$ detection are listed in Table 3 of Paper I with upper limits on L_{IR} . For these objects $L_{\text{IR}} \lesssim 0.3 \times 10^{44} \text{ erg s}^{-1}$, and corresponding SFRs are lower than $\lesssim 1 M_{\odot} \text{ yr}^{-1}$.

are flagged as possible AGNs. Given the expected dispersion, the rough agreement between the SFRs is consistent with the IR emission being dominated by star formation.

3.1. Caveat: The Dust-to-Gas Ratio

The derived SFR might be underestimated if the cold gas in the BCGs has a low dust-to-gas ratio. This might be the case if the gas has cooled from the hot ICM and if the dust was destroyed while

TABLE 3
COMPARISON OF ESTIMATES OF STAR FORMATION RATE

BCG (1)	OD08 (2)	C99 (3)	HM05 (4)	MO93 (5)	M95 (6)	M04 (7)	M05 (8)	B03 (9)	MO89 (10)	OD04 (11)	D07 (12)
A262.....	0.5			0.02							
A2597.....				12						10	4
A1795.....		2	9	12					1.8	10	
A1835.....		77–125	123				100				
A1835.....							138 (FIR)				
Hydra A.....			9.5		1 (b)						
Hydra A.....					23–35 (c)						
A2052.....	1.4	0.96						0.4–0.6	0.16		
A1068.....	188	30				16–40					
A1068.....						68 (IR)					
A1664.....	14	23									
R1532.....	97	12									
A2146.....	192	5.6									
PKS 0745.....	17		129								

NOTES.—Comparison of SFRs from this paper (col. [2]) with estimates from the literature (cols. [3]–[12]). Values are in units of $M_{\odot} \text{ yr}^{-1}$. References are as follows: OD08, this paper; C99, Crawford et al. (1999); HM05, Hicks & Mushotzky (2005); MO93, McNamara & O’Connell (1993); M95, McNamara (1995); M04, McNamara et al. (2004); M05, McNamara et al. (2006); B03, Blanton et al. (2003); MO89, McNamara & O’Connell (1989); OD04, O’Dea et al. (2004); D07, Donahue et al. (2007b). For Hydra A, (b) and (c) refer to “short-duration burst” and “continuous star formation models,” respectively.

in the hot phase and there has not been sufficient time to form dust at the levels typically seen in normal star-forming galaxies. However, there are several arguments against a low gas-to-dust ratio: (1) The observations of H_2 (e.g., Donahue et al. 2000; Edge et al. 2002; Hatch et al. 2005; Jaffe et al. 2005; Egami et al. 2006a; Johnstone et al. 2007) and CO (Edge 2001; Salomé & Combes 2003, 2004) associated with the BCG optical emission-line nebulae require the presence of significant amounts of dust to shield the molecular gas. (2) Dust is clearly seen in the optical emission-line nebulae in cool core clusters (e.g., Sparks et al. 1989, 1993; McNamara & O’Connell 1992; Donahue & Voit 1993;

Koekemoer et al. 1999). (3) Studies of the nebulae in the BCGs of cool core clusters suggest the presence of dust-to-gas ratios consistent with Galactic values (Sparks et al. 1989, 1993; Donahue & Voit 1993). (4) Theoretical arguments suggest that dust could form quickly inside cool clouds (Fabian et al. 1994; Voit & Donahue 1995).

4. COMPARISON BETWEEN IR LUMINOSITY AND X-RAY LUMINOSITY

The integrated X-ray luminosity of a cluster is dependent on the combination of its core and larger scale structure. As such, any correlation between this global property and the properties of the BCG may indicate an underlying link, particularly as our sample from its selection will favor cool cores. Therefore, we plot the X-ray luminosity of the host cluster (listed in Table 1 of Paper I) against estimated IR luminosities for all BCGs with color ratio $F_{8 \mu\text{m}}/F_{5.8 \mu\text{m}} > 0.75$ in Figure 2. In Figure 3 we show X-ray luminosities compared to the color $F_{8 \mu\text{m}}/F_{5.8 \mu\text{m}}$. This study covers a much larger range in X-ray luminosity than Egami et al.

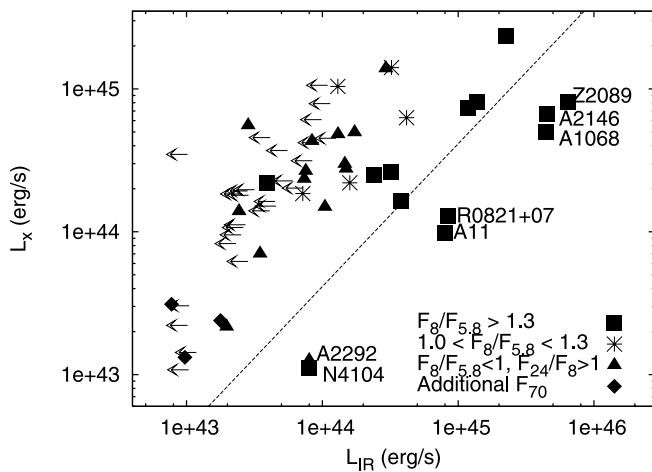


FIG. 2.—X-ray luminosity vs. estimated IR luminosity. X-ray and IR luminosities are listed in Tables 1 and 3 of Paper I. Squares represent our reddest group, with $8 \mu\text{m}$ -to- $5.8 \mu\text{m}$ flux ratios greater than 1.3. The intermediate group, with flux ratios between 1.0 and 1.3, are plotted as asterisks. Triangles have $8 \mu\text{m}$ -to- $5.8 \mu\text{m}$ flux ratios less than 1 but $24 \mu\text{m}$ -to- $8 \mu\text{m}$ flux ratios above 1. Diamonds represent galaxies with both $24 \mu\text{m}$ -to- $8 \mu\text{m}$ and $8 \mu\text{m}$ -to- $5.8 \mu\text{m}$ flux ratios less than 1 but have been detected at $70 \mu\text{m}$. Flux ratios are computed using photometry listed in Table 2 in Paper I. Upper limits on the IR luminosity are shown by arrows. We find a weak correlation between X-ray and IR luminosity. The dashed line shows the kinetic energy injection rate predicted from a star-forming population due to supernovae as a function of the IR luminosity. We confirm that kinetic energy from supernovae cannot account for the X-ray radiative energy losses in most cooling flows.

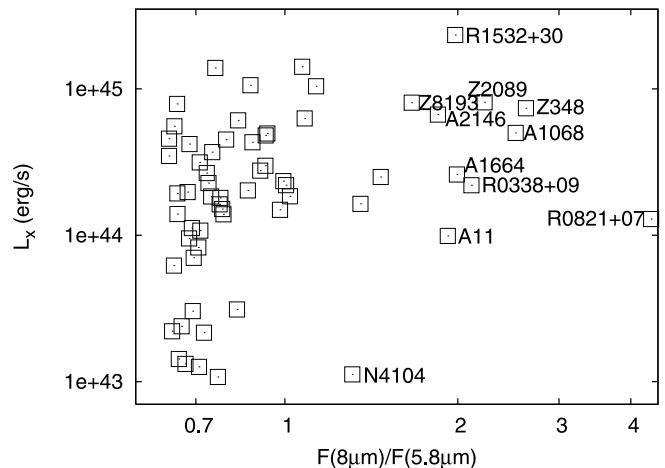


FIG. 3.—X-ray luminosity vs. $8 \mu\text{m}$ -to- $5.8 \mu\text{m}$ flux ratio (data taken from Tables 1 and 2 in Paper I). Most red objects with $F_{8 \mu\text{m}}/F_{5.8 \mu\text{m}} > 1$ have X-ray luminosity $L_X > 10^{44} \text{ erg s}^{-1}$.

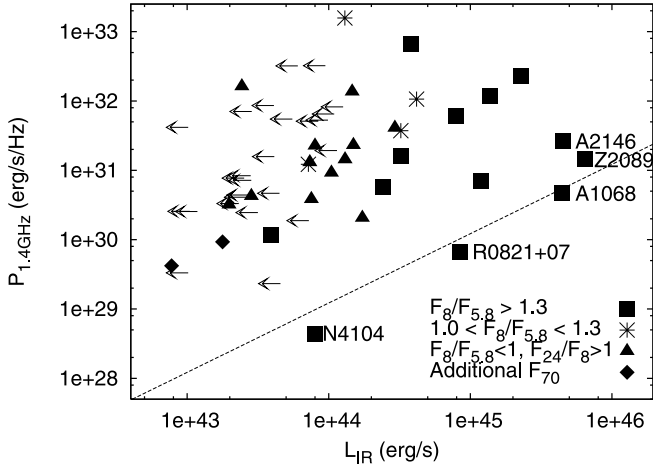


FIG. 4.—Radio luminosity at 1.4 GHz (listed in Table 1 of Paper I) vs. estimated IR luminosity (Table 2). The radio-IR correlation (eq. [2]) for star-forming objects is shown as a dashed line. The radio fluxes are much higher than expected from the radio-IR correlation appropriate for star-forming late-type galaxies. This is not unexpected, since many of these objects contain radio cores and in some cases even double-lobed jets. We find a weak correlation between the radio luminosity at 1.4 GHz and the IR luminosity. The symbols are the same as in Fig. 2.

(2006b). We see that BCGs with higher IR luminosity and redder $8\ \mu\text{m}$ – $5.8\ \mu\text{m}$ colors (indicating an IR excess) tend to have higher X-ray luminosities. However, there are many objects with high X-ray luminosity ($L_X > 10^{44}\ \text{erg s}^{-1}$) that do not have an IR excess.

It is interesting to compare the kinetic energy injected by supernovae (from an SFR consistent with the IR luminosity) to the energy radiated in X-rays. Leitherer et al. (1999) estimate a mechanical energy of about $10^{42}\ \text{erg s}^{-1}$ normalized for an SFR of $1\ M_{\odot}\ \text{yr}^{-1}$. These conversion factors have been used to estimate the mechanical energy due to supernovae as a function of IR luminosity. This relation is shown in Figure 2 (*dashed line*). We see that there are a few BCGs for which there may be sufficient mechanical energy to resupply the X-ray luminosity. However, in general, for the sample as a whole, we confirm the finding of previous studies (e.g., McNamara et al. 2006) that mechanical energy input from supernovae is not sufficient (by a few orders of magnitude) to account for the current radiative energy losses of the ICM as a whole or in the core.

5. COMPARISON TO RADIO LUMINOSITY

We find a modest (almost $3\ \sigma$) correlation between the IR luminosity and the radio luminosity at 1.4 GHz (as we show in Fig. 4). We compare the radio fluxes to those appropriate for star-forming objects with a dashed line in the lower right portion of Figure 4. The radio-IR relation for star-forming objects (eq. [3] of Bell 2003) is

$$\left(\frac{L_{1.4\ \text{GHz}}}{\text{erg cm}^{-2}\ \text{s}^{-1}\ \text{Hz}^{-1}}\right) = \left(\frac{L_{\text{IR}}}{3.75 \times 10^{12+q}\ \text{erg cm}^{-2}\ \text{s}^{-1}\ \text{Hz}^{-1}}\right), \quad (2)$$

where q is a logarithmic index. We have used the mean value $q = 2.34$ by Yun et al. (2001).

In Figure 4 the majority of radio fluxes are well above this relation. The three objects below the line are (*left to right*) NGC 4104, R0821+07, and A1068. NGC 4104 is nearer than the other objects in the survey, and it is possible that the $H\alpha$ flux and radio

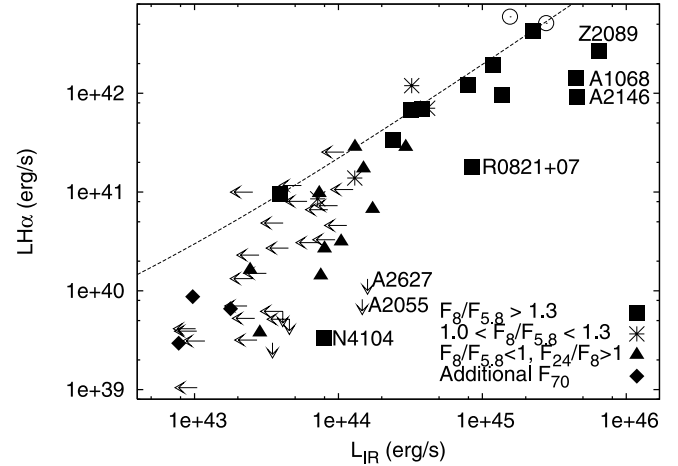


FIG. 5.—Observed $H\alpha$ luminosity (listed in Table 1 of Paper I) vs. infrared luminosity estimated from the $8\ \mu\text{m}$ and $24\ \mu\text{m}$ fluxes. The data for two BCGs from Egami et al. (2006a) are shown as open circles. The Kennicutt relation inferred from observations of star-forming galaxies relating $H\alpha$ luminosity to SFR is plotted as a dotted line. We have divided the line by a factor of 2.8 to remove the reddening correction, since our $H\alpha$ luminosities are uncorrected for reddening. The $H\alpha$ fluxes are consistent with the estimated IR luminosities and star formation. As in Fig. 2, the symbols depend on the $8\ \mu\text{m}$ – $5.8\ \mu\text{m}$ color. We suspect that some of the $H\alpha$ luminosities are lower than expected because the apertures used to measure them were smaller than those used to measure the IR fluxes.

flux density have been underestimated. The other two clusters (A1068 and R0821+07) have $F_{8\ \mu\text{m}}/F_{5.8\ \mu\text{m}} > 1.3$ and have unresolved red sources seen in the IRAC color maps and so are likely to be dominated by an AGN.

Thus, the BCGs (independent of whether they have an IR excess) tend to have radio emission which is dominated by that produced by an AGN. Based on hot IR colors and high $[\text{O III}]/H\beta$ ratios it appears that only four of the BCGs host a type II AGN with a luminous accretion disk (Paper I). Thus, either the AGNs in most of the BCGs are currently turned off, or they are accreting in a low-luminosity mode. The (weak) correlation between radio and IR luminosity may be a consequence of the correlation between mass accretion rate and SFR (§ 8); i.e., the cooling gas feeds the AGN and makes gas available for star formation. In addition, the ratio of mechanical energy in the radio source outflow to the radio luminosity can vary by about 3 orders of magnitude (Birzan et al. 2004). Thus, the radio luminosity can be a poor measure of the impact of the radio source on its environment.

6. COMPARISON TO $H\alpha$ LUMINOSITY

We compare the $H\alpha$ luminosities from limited-aperture spectroscopy to the IR luminosities in Figure 5, finding a strong correlation between the two. We also see a correlation in $H\alpha$ flux versus $24\ \mu\text{m}$ flux density (Fig. 6). These correlations show that the $H\alpha$ and IR emission arises from the same or a related power source. We suggest that the dominant power source for the $H\alpha$ and IR emission is star formation. This is consistent with previous evidence that the optical emission-line nebulae are mostly powered by UV photons from young stars with a possible secondary contribution from another mechanism (e.g., Johnstone & Fabian 1988; Allen 1995; Voit & Donahue 1997; Crawford et al. 1999; O’Dea et al. 2004; Wilman et al. 2006; Hatch et al. 2007). The $H\alpha$ -SFR law relating the SFR to the $H\alpha$ luminosity,

$$\text{SFR}(M_{\odot}\ \text{yr}^{-1}) = \frac{L(H\alpha)}{1.26 \times 10^{41}\ \text{erg s}^{-1}} \quad (3)$$

can be accommodated in terms of the observed molecular gas (Edge 2001) or observed SFRs (Table 3). More plausibly, hot gas mixing with dusty cold gas is the source of 10%–20% of the IR emission. In this case our results allow for modest mass cooling rates of up to tens to hundreds of $M_{\odot} \text{ yr}^{-1}$, comparable to the range shown in Table 3.

Cosmic rays also fail as an energy source, unless they are recycled. Since $L_{\text{IR}} \sim L_{\text{cool}}$ (to within about a factor of 3; see Fig. 11), the energy required for the IR is comparable with the thermal energy within r_{cool} . Consequently, the cosmic-ray pressure would need to be high, with a pressure $P_{\text{CR}} = f_{\text{CR}} P_{\text{Th}}$ with $f_{\text{CR}} > 0.3$ and thermal pressure P_{Th} . This is contrary to the quasi-hydrostatic appearance of the ICM in cluster cores.

Only if there is some efficient mechanism for energy to flow from the central accretion flow/AGN to the dust can an alternative be viable. In the absence of any such mechanism, we conclude that the UV radiation from massive star formation must be the energy source for the mid-IR emission measured by *Spitzer*.

9. SUMMARY

Paper I obtained *Spitzer* photometry of a sample of 62 BCGs in X-ray-bright clusters selected on the basis of BCG $H\alpha$ flux, which tends to favor cool core clusters. They showed that at least half of the BCGs exhibit an IR excess with a luminosity $L_{\text{IR}} \sim 10^{43}$ – $\text{few} \times 10^{45} \text{ erg s}^{-1}$. In this paper we examined correlations in the data and discussed implications for cool core clusters.

BCGs with an IR excess are found mainly in clusters at high X-ray luminosity ($L_X > 10^{44} \text{ erg s}^{-1}$). But not all high- L_X clusters have a BCG with an IR excess.

The IR luminosity is proportional to the $H\alpha$ luminosity, suggesting that they are powered by the same or a related source of energy. We suggest that star formation is the dominant power source for the IR and $H\alpha$ emission. The $H\alpha$ luminosity falls below the Kennicutt (1998) relation probably because the spectroscopic apertures exclude much of the extended emission-line nebulae. The inferred star formation rates (SFRs) estimated from the IR luminosity are in the range of about 1–50 $M_{\odot} \text{ yr}^{-1}$. In most BCGs, supernovae produced by star formation with this SFR cannot account for the X-ray luminosity and so cannot be responsible for reheating the ICM.

The radio emission in the BCG is dominated by that produced by an AGN rather than star formation. However, there is a mod-

est correlation between radio and IR emission. This suggests the feeding of the AGN and the fueling of the star formation may have a common origin, perhaps gas cooling from the hot ICM.

The mass of molecular gas (estimated from CO observations) is correlated with the IR luminosity as found for normal star-forming galaxies. The gas depletion timescale is about 1 Gyr. Given that clusters are relatively young (perhaps 4–6 Gyr since the last major merger), it is possible that there may have been insufficient time for a complete steady state (cooling leads to cold gas leads to star formation) to be set up.

We fit a Schmidt-Kennicutt relation to the molecular gas mass versus SFR and estimate a rough star-forming region diameter. For most BCGs the implied sizes of 10–20 kpc are comparable to those of the color variations seen in the IRAC data and to the optical emission-line nebulae. This is consistent with the hypothesis that star formation occurs in molecular gas associated with the emission-line nebulae and with evidence that the emission-line nebulae are mainly powered by ongoing star formation.

BCGs in clusters with shorter cooling times for the hot ICM have higher IR luminosities. We find a strong correlation between mass deposition rates (\dot{M}_X) estimated from the X-ray emission and the SFR. The SFR is about 30–100 times smaller than \dot{M}_I , the mass accretion rate derived from imaging, and 3–10 times smaller than \dot{M}_S , the rate derived from spectroscopy. The observed trends between cooling time and IR luminosity and between \dot{M}_S and the IR SFRs are consistent with the hypothesis that the cooling ICM is the source of the gas which is forming stars. The correlation between mass deposition rates estimated from the X-ray radiative losses and the SFRs suggests that the fraction of gas that does cool is set by the balance of heating and cooling by the cooling flow. The low value of SFR/\dot{M}_X suggests that heating is likely to be very efficient in preventing most of the gas at temperatures of a few keV from cooling further.

This work is based in part on observations made with the *Spitzer Space Telescope*, which is operated by the Jet Propulsion Laboratory, California Institute of Technology, under a contract with NASA. Support for this work at the University of Rochester and Rochester Institute of Technology was provided by NASA through an award issued by JPL/Caltech. We are grateful to the referee for helpful comments.

REFERENCES

- Allen, S. W. 1995, *MNRAS*, 276, 947
 Arnaud, K. 1996, in ASP Conf. Ser. 101, *Astronomical Data Analysis Software and Systems V*, ed. G. H. Jacoby & J. Barnes (San Francisco: ASP), 17
 Baum, S. A., Heckman, T. M., Bridle, A., van Breugel, W. J. M., & Miley, G. K. 1988, *ApJS*, 68, 643
 Baum, S. A., & O'Dea, C. P. 1991, *MNRAS*, 250, 737
 Bell, E. F. 2003, *ApJ*, 586, 794
 Best, P. N., von der Linden, A., Kauffmann, G., Heckman, T. M., & Kaiser, C. R. 2007, *MNRAS*, 379, 894
 Birzan, L., Rafferty, D. A., McNamara, B. R., Wise, M. W., & Nulsen, P. E. J. 2004, *ApJ*, 607, 800
 Blanton, E. L., Sarazin, C. L., & McNamara, B. R. 2003, *ApJ*, 585, 227
 Böhringer, H., Matsushita, K., Churazov, E., Ikebe, Y., & Chen, Y. 2002, *A&A*, 382, 804
 Calzetti, D. 2008, *Nuovo Cimento*, in press (arXiv: 0801.2558)
 Cardiel, N., Gorgas, J., & Aragon-Salamanca, A. 1998, *Ap&SS*, 263, 83
 Cowie, L. L., & Binney, J. 1977, *ApJ*, 215, 723
 Cowie, L. L., Hu, E. M., Jenkins, E. B., & York, D. G. 1983, *ApJ*, 272, 29
 Crawford, C. S., Allen, S. W., Ebeling, H., Edge, A. C., & Fabian, A. C. 1999, *MNRAS*, 306, 857
 Crawford, C. S., & Fabian, A. C. 1992, *MNRAS*, 259, 265
 ———. 1993, *MNRAS*, 265, 431
 Donahue, M., Mack, J., Voit, G. M., Sparks, W., Elston, R., & Maloney, P. R. 2000, *ApJ*, 545, 670
 Donahue, M., Stocke, J. T., & Gioia, I. 1992, *ApJ*, 385, 49
 Donahue, M., Sun, M., O'Dea, C. P., Voit, G. M., & Cavagnolo, K. W. 2007a, *AJ*, 134, 14
 Donahue, M., & Voit, G. M. 1993, *ApJ*, 414, L17
 Donahue, M., et al. 2007b, *ApJ*, 670, 231
 Dunn, R. J. H., & Fabian, A. C. 2006, *MNRAS*, 373, 959
 Dunn, R. J. H., Fabian, A. C., & Taylor, G. B. 2005, *MNRAS*, 364, 1343
 Dwek, E. 1986, *ApJ*, 302, 363
 Dwek, E., Rephaeli, Y., & Mather, J. C. 1990, *ApJ*, 350, 104
 Edge, A. C. 2001, *MNRAS*, 328, 762
 Edge, A. C., Stewart, G. C., & Fabian, A. C. 1992, *MNRAS*, 258, 177
 Edge, A. C., Wilman, R. J., Johnstone, R. M., Crawford, C. S., Fabian, A. C., & Allen, S. W. 2002, *MNRAS*, 337, 49
 Edwards, L. O. V., Hudson, M. J., Balogh, M. L., & Smith, R. J. 2007, *MNRAS*, 379, 100
 Egami, E., Rieke, G. H., Fadda, D., & Hines, D. C. 2006a, *ApJ*, 652, L21
 Egami, E., et al. 2006b, *ApJ*, 647, 922
 Fabian, A. C. 1994, *ARA&A*, 32, 277
 Fabian, A. C., Johnstone, R. M., & Daines, S. J. 1994, *MNRAS*, 271, 737
 Fabian, A. C., & Nulsen, P. E. J. 1977, *MNRAS*, 180, 479

- Fabian, A. C., et al. 2002, MNRAS, 335, L71
———. 2006, MNRAS, 366, 417
- Hansen, L., Jorgensen, H. E., & Norgaard-Nielsen, H. U. 1995, A&A, 297, 13
- Hansen, L., Jorgensen, H. E., Norgaard-Nielsen, H. U., Pedersen, K., Goudfrooij, P., & Linden-Vornle, M. J. D. 2000, A&A, 356, 83
- Hatch, N. A., Crawford, C. S., & Fabian, A. C. 2007, MNRAS, 380, 33
- Hatch, N. A., Crawford, C. S., Fabian, A. C., & Johnstone, R. M. 2005, MNRAS, 358, 765
- Heckman, T. M. 1981, ApJ, 250, L59
- Heckman, T. M., Baum, S. A., van Breugel, W. J. M., & McCarthy, P. 1989, ApJ, 338, 48
- Hicks, A. K., & Mushotzky, R. 2005, ApJ, 635, L9
- Hu, E. M. 1992, ApJ, 391, 608
- Hutchings, J. B., & Balogh, M. L. 2000, AJ, 119, 1123
- Jaffe, W., Bremer, M. N., & Baker, K. 2005, MNRAS, 360, 748
- Jaffe, W., Bremer, M. N., & van der Werf, P. P. 2001, MNRAS, 324, 443
- Johnstone, R. M., & Fabian, A. C. 1988, MNRAS, 233, 581
- Johnstone, R. M., Fabian, A. C., & Nulsen, P. E. J. 1987, MNRAS, 224, 75
- Johnstone, R., Hatch, N., Ferland, G., Fabian, A., Crawford, C., & Wilman, R. 2007, MNRAS, 382, 1246
- Kaastra, J. S., Ferrigno, C., Tamura, T., Paerels, F. B. S., Peterson, J. R., & Mittaz, J. P. D. 2001, A&A, 365, L99
- Kaiser, C. R., & Binney, J. 2003, MNRAS, 338, 837
- Kalberla, P. M. W., Burton, W. B., Hartmann, D., Arnal, E. M., Bajaja, E., Morras, R., & Poppel, W. G. L. 2005, A&A, 440, 775
- Kennicutt, R. C., Jr. 1998, ApJ, 498, 541
- Koekemoer, A. M., O'Dea, C. P., Sarazin, C. L., McNamara, B. R., Donahue, M., Voit, G. M., Baum, S. A., & Gallimore, J. F. 1999, ApJ, 525, 621
- Leitherer, C., et al. 1999, ApJS, 123, 3
- McNamara, B. R. 1995, ApJ, 443, 77
———. 2004, in Proc. Riddle of Cooling Flows in Galaxies and Clusters of Galaxies, ed. T. Reiprich, J. Kempner, & N. Soker, <http://www.astro.virginia.edu/coolflow/>
- McNamara, B. R., & Nulsen, P. E. J. 2007, ARA&A, 45, 117
- McNamara, B. R., & O'Connell, R. W. 1989, AJ, 98, 2018
———. 1992, ApJ, 393, 579
———. 1993, AJ, 105, 417
- McNamara, B. R., Wise, M. W., & Murray, S. S. 2004, ApJ, 601, 173
- McNamara, B. R., et al. 2006, ApJ, 648, 164
- Mittaz, J. P. D., et al. 2001, A&A, 365, L93
- Narayan, R., & Medvedev, M. 2001, ApJ, 562, L129
- O'Dea, C. P., Baum, S. A., & Gallimore, J. F. 1994, ApJ, 436, 669
- O'Dea, C. P., Baum, S. A., Mack, J., Koekemoer, A. M., & Laor, A. 2004, ApJ, 612, 131
- Oegerle, W. R., et al. 2001, ApJ, 560, 187
- Omma, H., Binney, J., Bryan, G., & Slyz, A. 2004, MNRAS, 348, 1105
- Peterson, J. R., & Fabian, A. C. 2006, Phys. Rep., 427, 1
- Peterson, J. R., Kahn, S. M., Paerels, F. B. S., Kaastra, J. S., Tamura, T., Bleeker, J. A. M., Ferrigno, C., & Jernigan, J. G. 2003, ApJ, 590, 207
- Peterson, J. R., et al. 2001, A&A, 365, L104
- Quillen, A., et al. 2008, ApJS, 176, 39 (Paper I)
- Rafferty, D. A., McNamara, B. R., Nulsen, P. E. J., & Wise, M. W. 2006, ApJ, 652, 216
- Read, A. M., & Ponman, T. J. 2003, A&A, 409, 395
- Romanishin, W. 1987, ApJ, 323, L113
- Ruszkowski, M., & Begelman, M. 2002, ApJ, 581, 223
- Salomé, P., & Combes, F. 2003, A&A, 412, 657
———. 2004, A&A, 415, L1
- Sanders, J. S., & Fabian, A. C. 2007, MNRAS, 381, 1381
- Sanders, J. S., Fabian, A. C., Allen, S. W., Morris, R. G., Graham, J., & Johnstone, R. M. 2008, MNRAS, 385, 1186
- Smith, E. P., Bohlin, R. C., Bothum, G. D., O'Connell, R. W., Roberts, M. S., Neff, S. G., Smith, A. M., & Stecher, T. P. 1997, ApJ, 478, 516
- Soker, N., Blanton, E. L., & Sarazin, C. L. 2002, ApJ, 573, 533
- Sparks, W. B., Ford, H. C., & Kinney, A. L. 1993, ApJ, 413, 531
- Sparks, W. B., Macchetto, F., & Golombek, D. 1989, ApJ, 345, 153
- Tamura, T., et al. 2001, A&A, 365, L87
- Tucker, W. H., & David, L. P. 1997, ApJ, 484, 602
- Voigt, L. M., Schmidt, R. W., Fabian, A. C., Allen, S. W., & Johnstone, R. M. 2002, MNRAS, 335, L7
- Voit, G. M., & Donahue, M. 1995, ApJ, 452, 164
———. 1997, ApJ, 486, 242
- Wilman, R. J., Edge, A. C., & Swinbank, A. M. 2006, MNRAS, 371, 93
- Young, J. S., Schloerb, F. P., Kenney, J. D., & Lord, S. D. 1986, ApJ, 304, 443
- Yun, M. S., Reddy, N. A., & Condon, J. J. 2001, ApJ, 554, 803

